

HSU, CHIA-CHI, M.S. Expression of *Wnt5a* Alternative Promoters A and B During Cancer Progression and Cellular Differentiation. (2012)

Directed by Dr. Karen S. Katula. 55 pp.

WNT5A is a secreted glycoprotein that plays an important role in cellular differentiation, cell homeostasis and development. It is also misregulated in numerous cancer cell types. The *Wnt5a* gene generates multiple transcripts from distinct promoters and alternative splicing, leading to different protein isoforms. Currently, little is known regarding the regulation of the *Wnt5a* alternative promoters. The goal of this study was to characterize the expression of *Wnt5a* alternative promoters A and B during differentiation and cellular transformation. TaqMan primer-probe sets, specific to promoter A and promoter B derived transcripts, were designed and characterized. The level of promoter A and B specific transcripts were determined in normal human osteoblasts and the osteosarcoma cell line, SaOS-2, as a model for cancer progression. The level of promoter A and B transcripts were nearly equal in osteoblasts cells. In contrast, there was a dramatic decrease in promoter B transcripts in osteosarcoma cells and an increase of 3.5 fold in promoter A transcripts, giving an A to B ratio of 2320 to 1. *Wnt5a* promoter A and promoter B luciferase reporter constructs were transfected into osteosarcoma cells. Promoter A and promoter B activities were found to be nearly equal, suggesting that the lower level of promoter B transcripts in osteosarcoma cells is not due to altered levels of transcription factors. Promoter A and promoter B specific transcripts were assayed in 3T3-L1 mouse fibroblasts, as a model for differentiation, in the following stages: exponential preadipocytes (EX PA), confluent preadipocytes (CON PA), two days after MDI treatment (D2 Post MDI) and in mature differentiated

adipocytes (Diff AD). In EX PA and CON PA cells, both promoter A and promoter B transcripts increased followed by decreased transcript levels in D2 Post MDI cells. While promoter A transcripts slightly increased in Diff AD, promoter B transcript levels remained at a low level. Overall, these results suggest that *Wnt5a* promoter A and promoter B are differentially regulated.

EXPRESSION OF *WNT5A* ALTERNATIVE PROMOTERS A AND B DURING
CANCER PROGRESSION AND CELLULAR DIFFERENTIATION

by

Chia-Chi Hsu

A Thesis Submitted to
the Faculty of The Graduate School at
The University of North Carolina at Greensboro
in Partial Fulfillment
of the Requirements for the Degree
Master of Science

Greensboro
2012

Approved by

Committee Chair

To my parents, who have supported and encouraged me
to pursue my dreams.

APPROVAL PAGE

This thesis has been approved by the following committee of the Faculty of The Graduate School at The University of North Carolina at Greensboro.

Committee Chair _____

Committee Members _____

Date of Acceptance by Committee

Date of Final Oral Examination

ACKNOWLEDGMENTS

First, I would like to thank my advisor, Dr. Karen Katula for her patience, support and encouragement during my graduate research experience. This thesis would not have been possible without her guidance and dedication.

I would like to show my gratitude to my committee members, Dr. Robert Cannon and Dr. David Remington for their time and suggestions. I would also like to acknowledge Dr. Patel for her knowledge and advice and providing cells used in this study.

I would like to extend my thanks to Dr. Ron Morrison from the Department of Nutrition for assisting my research by providing RNA samples. In addition, I would also like to thank former and present member of the lab, Nicole Joyner-Powell and Shannon Smith, for their contribution to this research.

Lastly, I would like to thank my family for their support and encouragement in my entire educational experience.

TABLE OF CONTENTS

	Page
LIST OF TABLES	vii
LIST OF FIGURES	viii
CHAPTER	
I. INTRODUCTION	1
Statement of problem	1
Wnt5a and signaling	2
Wnt5a and development	3
Wnt5a and mesenchymal stem cell differentiation	4
Wnt5a and cancer	5
Mechanism of Wnt5a misregulation in cancer	6
The Wnt5a gene structure and alternative promoters	7
3T3-L1 cell line and adipogenesis	8
Project overview	9
II. MATERIALS AND METHODS	12
Cell line and cell cultures	12
Differentiation of 3T3-L1 into adipocytes	12
RNA isolation and cDNA synthesis	13
Primer-probe selection and characterization	14
Real time quantitative PCR (qRT-PCR)	15
Determination of amplification efficiency	16
Analysis of promoter A and promoter B specific transcripts during 3T3-L1 differentiation	17
Analysis of promoter A and promoter B specific transcripts in osteoblast and osteosarcoma	19
Transient transfection and luciferase assay	19
III. RESULTS	21
Custom design primer and probe sets	21
Mouse Wnt5a promoter A and promoter B transcript levels during differentiation of 3T3-L1 cells	29

Human Wnt5a alternative promoter A and promoter B transcript levels in osteoblasts and osteosarcoma cells.....	37
Activity of separated promoter A and promoter B in osteosarcoma cells.....	42
IV. DISCUSSION.....	45
Overview.....	45
Custom designed primer-probe sets for Wnt5a alternative promoter A and promoter B	46
Promoter A and promoter B are differentially regulated during 3T3-L1 differentiation	47
Wnt5a alternative promoter A and B are differentially regulated in osteoblast and osteosarcoma cells	49
Decrease in promoter B transcript levels in osteosarcoma cells is unlikely due to changes in transcription factors	50
Functional importance of the Wnt5a alternative promoters	51
REFERENCES	53

LIST OF TABLES

	Page
Table 1. Comparison of human and mouse <i>Wnt5a</i> Genes	10
Table 2. <i>Wnt5a</i> custom designed mouse and human primer-probe sets	25
Table 3. <i>Wnt5a</i> custom designed primer-probe amplification efficiency values	29
Table 4. Comparison of 3T3-L1 Set 1 and Set 2 transcript levels	32
Table 5. <i>Wnt5a</i> promoter A and promoter B specific transcripts in 0.25µg of osteoblast and osteosarcoma RNA	41

LIST OF FIGURES

	Page
Figure 1. Gene Structure of human (A) and mouse (B) alternative promoter A and promoter B transcript units.....	11
Figure 2. Location of mouse and human primer-probe sets in exon 1 (a or b) plus cDNA sequences	23
Figure 3. Wnt5a qRT-PCR product sizes	26
Figure 4. Custom designed <i>Wnt5a</i> primer-probe efficiency curves	28
Figure 5. Mouse <i>Wnt5a</i> promoter A and promoter B PCR standard curves.....	31
Figure 6. Promoter A and Promoter B transcript levels during the course of 3T3-L1 cellular differentiation, from preadipocytes to adipocytes	33
Figure 7. Mouse <i>Wnt5a</i> promoter A to promoter B transcript number ratios during differentiation of 3T3-L1 cells	34
Figure 8. Transcript numbers in 0.01µg of RNA derived from <i>Wnt5a</i> promoter A and promoter B during the course of 3T3-L1 differentiation, Set 2	36
Figure 9. Mouse <i>Wnt5a</i> promoters A to promoter B transcripts number ratios in 3T3-L1	37
Figure 10. Human <i>Wnt5a</i> specific promoter A and promoter B PCR standard curve	39
Figure 11. Number of <i>Wnt5a</i> promoter A and promoter B specific transcripts in osteoblasts and osteosarcoma RNA	40
Figure 12. Ratio of <i>Wnt5a</i> promoter A to promoter B transcripts in osteoblast and osteosarcoma RNA.....	41
Figure 13. <i>Wnt5a</i> human promoter A and promoter B luciferase reporter constructs.....	43

Figure 14. Relative activity levels of human *Wnt5a* promoter A and promoter B
deletion constructs in osteosarcoma, SaOS-2 cells44

CHAPTER I

INTRODUCTION

Statement of problem

Cancers are among the most prevalent diseases that continue to affect humans. Cancer cells are known for their highly proliferative profile, and many factors have been shown to contribute to the development of cancer, including genetic and non-genetic molecular alterations. Previous studies have shown that *Wnt5a* plays a role in several human cancers, including breast, colorectal, osteosarcoma, pancreatic, papillary thyroid, and melanoma (Katoh *et al.* 2009; Binder *et al.* 2008). *Wnt5a* expression is often misregulated in cancer cells and its increased expression has been associated with metastasizing cancer cells (Ripka *et al.* 2007). *Wnt5a* has been shown to be upregulated in pancreatic and melanoma cancer (Ripka *et al.* 2007; Weeraratna *et al.* 2002), whereas in colon and breast cancers *Wnt5a* was shown to be down regulated (Ying *et al.* 2008; Leris *et al.* 2005). The misregulation of *Wnt5a* appears to involve non-genetic rather than genetic changes. The mechanism for its misregulation is not clearly defined. To further current understanding of *Wnt5a* regulation, my project goal was to characterize the regulation of two alternative *Wnt5a* promoters in both normal and transformed cells and during cellular differentiation. This study is significant because it will provide insights

into the alteration of *Wnt5a* gene expression during cancer progression and further our understanding of normal *Wnt5a* regulation.

Wnt5a and signaling

WNT5a is a part of the WNT family, a group of cysteine-rich glycoproteins, that signals through the cell surface Frizzles transmembrane proteins. The Wnt signaling pathway plays a key role in cell proliferation, movement, differentiation, and polarity (Wang *et al.* 2009; Silver *et al.* 2009). The Wnt signaling pathways include the canonical (Wnt/beta-catenin) and non-canonical pathways (Silver *et al.* 2009).

The canonical pathway is activated by the binding of Wnt ligands to the Frizzles receptor and the low density lipoprotein related protein (LRP) co-receptor. The Frizzles family receptors are transmembrane proteins encoded by the gene *Frizzles* (FZD). Upon binding of Wnt ligands, beta-catenin is hypophosphorylated and translocated to the nucleus, where it binds to a family of transcription factors, lymphoid-enhancer-binding factor/T-cell-specific transcription factor (LEF/TCF), to activate target gene transcription (Nishita *et al.* 2010; Vidal-Puig *et al.* 2008).

The non-canonical pathways, also known as beta-catenin-independent, are activated through stimulating intracellular calcium (Calcium Pathway) and activating of phospholipase C (PLC) and protein kinase (PKC) (PLP/CE pathway) (Imagawa *et al.* 2008). However, the detailed downstream signaling pathways for the non-canonical pathway is still not well understood. *Wnt5a* is thought to signal through the non-

canonical pathway via activating Rho-GTPases RhoA and Rac (Binder *et al.* 2007). This pathway also exerts an antagonistic effect to the canonical pathway, but in recent literatures WNT5a has also been shown to signal in the canonical pathways (Nishita *et al.* 2010; Silver *et al.* 2009). As a result of its complex signaling pathways, it has been difficult to establish a model for the misregulation of *Wnt5a* in cancers.

Wnt5a and development

Wnt5a is involved in a variety of developmental and differentiation events. When *Wnt5a* was functionally inactivated in mice, the outgrowth of limbs were greatly affected where truncated limbs and underdeveloped digits were produced as a result of decreased mesenchymal progenitor cell proliferation (Yamaguchi *et al.* 1999). In one study, the expression of *Wnt5a* was critical in promoting differentiation of interneurons by targeting transcription factors Dlx homeogenes (Paina *et al.* 2011). In the case of *Wnt5a* deficiency, *Wnt5a* knockout mice displayed defects in the midbrain morphogenesis, such as impairment in midbrain elongation and rounded ventricle cavity (Anderson *et al.* 2008). Recent study also showed that *Wnt5a* deficient mice exhibit retardation in tooth development, leading to abnormal teeth formation (Lin *et al.* 2011). Collectively, these studies suggest the critical role of *Wnt5a* in cell proliferation and development.

Wnt5a and mesenchymal stem cell differentiation

Studies revealed that Wnt signaling pathways can determine the fate of mesenchymal stem cell differentiation into myoblasts, osteoblasts or preadipocytes (Vidal-Puig *et al.* 2008). As a member of the Wnt family, WNT5a appears to be an important regulator of mesenchymal stem cells differentiation into osteoblasts and preadipocytes. In one study, *Wnt5a* was shown to express at a higher level in human mesenchymal stem cells than preadipocytes (Bilkovski *et al.* 2010). While the absence of WNT5a was shown to abolish osteogenesis from human mesenchymal stem cells, the presence of WNT5a inhibits the determination of preadipocyte differentiation from human mesenchymal stem cells (Bilkovski *et al.* 2010). Another study indicated that *Wnt5a* expression is necessary for chondrocyte and osteoblast differentiation in mouse endochondral skeletal morphogenesis (Wu *et al.* 2003).

In the same mesenchymal cell lineage, *Wnt5a* has been shown to play an important role in promoting early stages of adipogenesis. One study showed that when *Wnt5a* expression is knocked down, adipogenesis is impaired in 3T3-L1 mouse fibroblasts. When 3T3-L1 cells were induced into preadipocytes, *Wnt5a* expression gradually decreased in the first 24 hours but increased after 4 days (Imagawa *et al.* 2008). Contrary to these findings, another study showed that *Wnt5a* levels remained unchanged when human mesenchymal stem cells were differentiated into adipocytes. Together, how *Wnt5a* expression is regulated during mesenchymal stem cell differentiation, including

adipogenesis is not well understood. Nor are there any published studies on differential usage of the alternative *Wnt5a* promoters.

Wnt5a and cancer

Wnt5a expression is altered in many cancers, showing both overexpression and downregulation. Previous studies indicated that *Wnt5a* is downregulated in colorectal cancer, leukaemias and neuroblastoma (Silver *et al.* 2009). Other studies showed that decreased expression of *Wnt5a* inhibits cell growth, migration, and invasiveness of breast carcinomas and prostate cancer cells (Jonsson *et al.* 2002; Bjartell *et al.* 2011).

Overexpression of *Wnt5a* has also been detected in many cancers associated with metastatic behavior, such as gastric cancer (Kurayoshi *et al.* 2006), melanoma skin cancer (Weeraratna *et al.* 2002), osteosarcoma (Enomoto *et al.* 2009) and pancreatic cancer (Ripka *et al.* 2007). When *Wnt5a* was constitutively expressed in a nonmetastatic melanoma cell line, the cell shapes changed to be thin and irregular, and showed increased motility and invasion. In contrast, when the *Wnt5a*/Frizzled-5 receptor signaling pathway was disrupted, the melanoma cells showed a significant decrease in their invasion (Weeraratna *et al.* 2002). While the level of *Wnt5a* transcripts was found to be increased in the osteosarcoma cell line, *Wnt5a* and its receptor Ror2 were demonstrated to increase the invasive properties of osteosarcoma in a later study (Yokota *et al.* 2003; Enomoto *et al.* 2009)

The paradoxical results from these studies suggest that Wnt5a can be either oncogenic or tumor suppressing, depending on the cancer types. In spite of the important role of Wnt5a misregulation in cancer, the molecular basis for *Wnt5a* overexpression and down regulation is not clearly understood.

Mechanism of Wnt5a misregulation in cancer

Based on current published data, Wnt5a expression during cancer progression does not involve genetic change; rather it could be due to non-genomic change, such as DNA methylation (Wang *et al.* 2007). *Wnt5a* has been detected in various cancer tissues, and the hypermethylation of WNT5a has been detected in early stages of colorectal cancer, myeloid and acute lymphoblastic leukemia (Roman-Gomez *et al.* 2007). On the contrary, Wnt5a has also been found to be hypomethylated in prostate cancer tissues (Wang *et al.* 2007).

Alternatively, evidence from the literature indicates the altered expression of *Wnt5a* in certain cancers involves specific signaling pathways and transcription factors. The overexpression of transcription factor, CUTL1, was found to promote cancer cell motility and invasiveness by binding to the Wnt5a regulatory sequence and upregulating the transcription (Michl *et al.* 2005; Ripka *et al.* 2007). Recent studies also showed that NF-kappaB and tumor necrosis factor-alpha (TNF-alpha) are involved in the increase of *Wnt5a* expression in bone marrow stromal cells (Rauner *et al.* 2011).

The Wnt5a gene structure and alternative promoters

Previous literatures revealed that alternative promoters are commonly used in human genes and the average human gene contains 3.1 promoters (Cheong *et al.* 2006; Turner *et al.* 2008). The common use of alternative promoters allows diverse gene regulations mechanisms to occur, initiating complex activities in the cell. One example from the literature is guanine nucleotide binding protein (GNBP). GNBP contains ten potential alternative promoters that generate transcripts and it has been shown to be involved in metabolic regulation and development (Weinstain *et al.* 2007). Fibroblast growth factor receptor 1 (FGFR1), a cancer driver gene, contains seven alternative promoters that are differentially expressed in several diseases including myeloid leukemia and myeloid hyperplasia (Roumiantsev *et al.* 2004). In spite of the growing interests in the use of alternative promoters, little is known about how they are differentially regulated. In relation to this study, nothing is known regarding the differential utilization of *Wnt5a* alternative promoters.

The human and mouse *Wnt5a* genes are compared in Table 1 and Figure 1. Both genes have five introns and share similar alternative promoters. The mouse *Wnt5a* generates six transcripts, whereas human generates eight transcripts. This study is focused on transcripts Wnt5a-201 and Wnt5a-005 for the human and Wnt5a-001 and Wnt5a-002 for the mouse. The structures of these transcripts are shown in Figure 1. The promoters associated with these transcripts as referred to as promoter A (201 and 001) and promoter B (005 and 002). These alternative transcripts give rise to proteins with

distinct N-termini. The promoter A transcript includes 15 and 20 additional amino acids for human and mouse, respectively (Table 1). Both promoter A and promoter B derived transcripts contain five exons, except the exon 1 sequences are unique to each transcription start site, A and B. As shown, promoter A (human and mouse) includes exon 1a, whereas promoter B includes exon 1b. These sequences can be used to generate unique primers for quantitative RT-PCR analysis.

3T3-L1 cell line and adipogenesis

As previously discussed, WNT5a is involved in mesenchymal cell differentiation, including adipogenesis. As a model for adipogenesis, we chose to use the mouse cell line 3T3-L1. Using these cells, we investigated the differential utilization of the *Wnt5a* alternative promoters A and B during differentiation. 3T3-L1 mouse fibroblasts belong to the mesenchymal stem cell lineage. Studies suggested that when mesenchymal stem cells differentiate into preadipocytes and become committed to the adipocyte lineage, they lose the ability to differentiate into other cells in the mesenchymal stem cell family, such as myoblasts and osteoblasts (Vidal-Puig *et al* 2008).

3T3-L1 cells can be grown in culture as preadipocytes at subconfluent levels. To induce differentiation, the cells are allowed to become confluent and grow two additional days. At this point, the cells are treated with a mixture of insulin, glucocorticoid, dexamethasone and 1-methyl-3-isobutyl xanthane (MIX). Insulin enhances the expression of transcription factor PPAR δ . MIX inhibits cAMP phosphodiesterase, which

in turn increases cAMP and ultimately increases transcription factor, C/EBP β , expression. The presence of the synthetic glucocorticoid, dexamethasone increases the level of C/EBP δ . All these transcription factors are required for adipogenesis. As a result, the confluent 3T3-L1 undergo two more cell divisions and differentiate into mature adipocytes.

Project overview

Wnt5a plays an important role in cellular development and differentiation and it has been shown to be misregulated in various cancers (Silver *et al.* 2009). The *Wnt5a* gene contains distinct alternative promoters that generate multiple transcripts and functional proteins. Although many studies have looked at the total *Wnt5a* transcripts, little is known about the regulation of the alternative promoters. The objective of this study is to examine the *Wnt5a* alternative promoter A and promoter B expression during cancer progression and cellular differentiation using osteoblasts, osteosarcoma and 3T3-L1 cells. In this study, we 1) selected the unique primer-probe sets that amplify *Wnt5a* promoter A and promoter B transcripts, 2) determined the transcript levels in osteoblasts, osteosarcoma and 3T3-L1, and 3) analyzed the activities of separated promoters A and B in osteosarcoma cells.

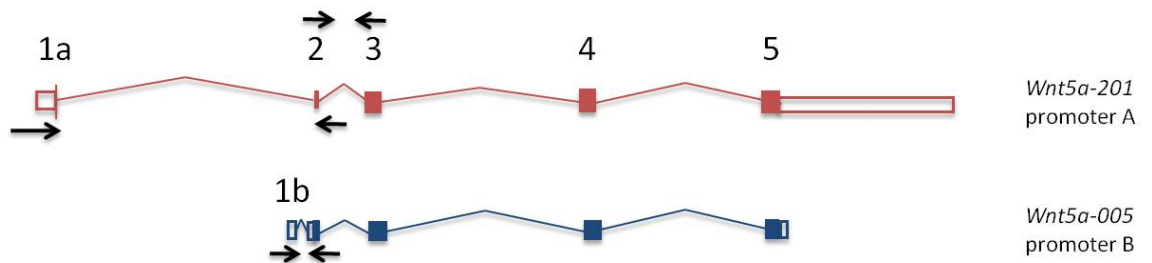
Table 1. Comparison of human and mouse *Wnt5a* genes

	Human	Mouse
Location	Chromosome #3 55, 499, 743-55, 523, 973 reverse	Chromosome #14 29, 317, 936-29, 340, 633 forward
Number of total Transcripts ²	8	6
Transcript size (Name) ³	6042 bp (WNT5A-201) 1299 bp (WNT5A-005)	7009 bp (Wnt5a-001) 3650 bp (Wnt5a-002)
Proteins Produced ²	6	2
Protein Length (AA) and ID ⁴	380 residues (ID #417310) 365 residues (ID #420104)	380 residues (ID #064878) 360 residues (ID #107891)
N-terminus of protein ^{3, 5}	<i>MKKSIGILSPGVALG (15)</i> MAGSAMSSKFFLVALAIFFS ...	<i>MKKPIGILSPGVALGTAGGA (20)</i> MSSKFFLMALATFFSFAQV V...
Exons and Introns (bp) ^{3,6}	<u>WNT5A-201</u> Exons: 324, 134, 251, 293, 4835 Introns: 6061, 1220, 4684, 3786 <u>WNT5A-005</u> Exons: #1b-63, #5-558 Introns: #1-412	<u>Wnt5a-001</u> Exons: 1365, 134, 251, 293, 4966 Introns: 5706, 1184, 4894, 3903 <u>Wnt5a-002</u> Exons: #1-19, #5-2953 Intron: #1-399

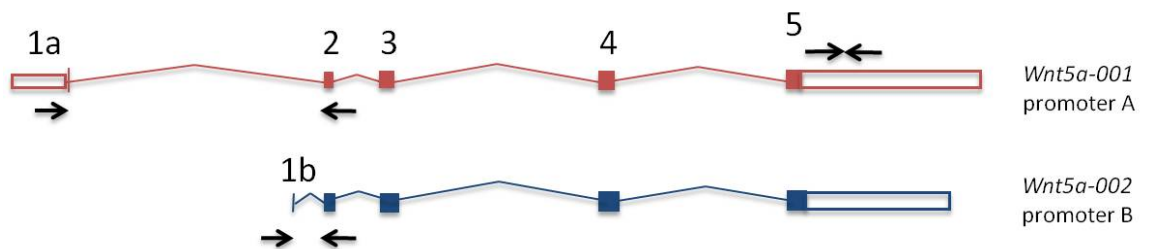
Source is from Ensemble: Human WNT5A ENSG00000114251 and Mouse Wnt5a ENSMUSG00000021994.² The total number of transcripts or proteins generated from the *Wnt5a* genomic region.³The two human and mouse transcripts that will be analyzed in this study. Transcript ID is preceded by ENST00000264634 for human or ENSMUST000000063465 for mouse.⁴ Protein lengths derived from the two transcripts that will be analyzed. ID number is preceded by ENSP000000497027 for human or ENSMUSO00000112272 for mouse.⁵Italicized amino acid (AA) sequence and the number in parenthesis indicate the additional AA's and N-terminus on the longer transcript (³). The AA sequence of the longer transcript includes all the AA's shown and is continuous. Bottom sequence includes the N-terminus and first 20 AA of the shorter transcript (³).⁶ Only the unique exons and introns for the shorter transcript are included; all others are identical to the longer transcript. (Modified from Katula *et al.* submitted)

Figure 1. Gene structure of human (A) and mouse (B) alternative promoter A and promoter B transcript units. The solid boxes indicate exon sequences. The lines are intron sequences. The open boxes are non-coding exon sequences. The arrows under the gene structure indicate the relative positions of the transcript primers proposed in this study. The arrows above the gene structure indicate the location of the commercial primers used to detect total Wnt5a transcripts.

A. Human



B. Mouse



CHAPTER II

MATERIAL AND METHODS

Cell line and cell cultures

In this study, mouse 3T3-L1 preadipocytes, mouse NIH3T3 fibroblasts and human osteosarcoma, SaOS-2, cell lines were utilized. The Set 1 3T3-L1 mouse fibroblast cell line was obtained from Dr. Yashomati Patel's lab (Biology, UNCG). The 3T3-L1 cells were grown in high glucose Dulbecco's modified Eagle's medium (DMEM) containing either 10% fetal bovine serum (FBS) or 10% calf bovine serum (CBS) and 1% penicillin/streptomycin (5000 I.U./mL and 5000 µg/mL), depending on the stage of differentiation. The NIH3T3 cells were grown in DMEM containing 10% calf bovine serum. The osteosarcoma cell line, SaOS-2, was obtained from the American Type Culture Collection (ATCC). The cells were grown in McCoy's 5a Medium containing 15% fetal bovine serum and 1% penicillin/streptomycin (5000 I.U./mL and 5000 µg/mL). All cells were cultured in a 37°C and 5% CO₂ humidified incubator.

Differentiation of 3T3-L1 into adipocytes

Initially, the cells were grown in DMEM medium containing 10% fetal bovine serum. For the purpose of adipocyte differentiation study, cells were fed with DMEM

medium containing 10% calf bovine serum and 1% penicillin/streptomycin (5000 units/ μ L and 5000 μ g/mL). To begin the adipocyte differentiation study, 3T3-L1 cells plated in a T-75 flask were grown to approximately 80% confluency. The cells were collected with trypsin treatment and replated in ten 10 cm dishes. When the cells were approximately 60% confluent, one plate of cells was used for RNA isolation. These cells were labeled “exponential preadipocyte” (EX PA). After the cells reached approximated 90% confluency on day 3, the medium was changed and the cells were grown for two additional days. RNA was isolated from cells on the first day of the two days. These served as the time point for “confluent preadipocytes” (CON PA). The remaining cells at two days post confluent were treated with MDI to promote differentiation.

MDI contains 5 μ M of 3-isobutyl 1-methyl-xanthine, 1.7 nM insulin and 1 nM dexamethasone. RNA was isolated from cells two days after MDI treatment. This sample represents the two day post MDI (D2 Post MDI) RNA. After the two days treatment with MDI, the medium was removed and replaced with DMEM containing 10% fetal bovine serum plus 0.45 nM of insulin. The cells were allowed to grow until differentiation was apparent. For Set 1, RNA was isolated from differentiated adipocytes on day 7, following MDI treatment. This sample represents the “Diff AD” RNA.

RNA isolation and cDNA synthesis

In this study, RNA was isolated from different cultured cells (3T3-L1, NIH3T3 and SaOS-2) with the SV Total RNA Isolation System (Promega, Inc). First, the medium

was removed from the cells and 5 mL of phosphate-buffer saline (PBS) was added and removed. In some experiments, 5 mL PBS was added to the cells and the cells were scraped from the plate. The cell solution was centrifuged for 5 minutes at setting number 4 in a clinical centrifuge. The PBS was removed and the cell pellet was quickly frozen in liquid nitrogen and stored at -80 °C. In other experiments, 175 µL of the RNA Lysis Buffer from the RNA isolation kit was added to the pelleted cells and resuspended. The cell lysate was stored at -80 °C.

For the RNA isolation, the frozen cell pellets were resuspended in 175 µL RNA Lysis Buffer. The frozen cell lysates already in the RNA Lysis Buffer were allowed to thaw on ice. From this point on, the procedure was identical, following the manufacturer's protocol.

The concentration and quality of the RNA were determined by reading the optical density (O.D.) values at 260 nm and 280 nm of 2 µL purified RNA, utilizing a nanodrop plate reader and the TakeThree Session program from the Gene5™ BioTek (Synergy2) reader. 1-3 µg of RNA was converted to cDNA using the QuantiTech Reverse Transcription Kit (Qiagen) or Maxima First Strand cDNA Synthesis Kit (Fermenta Life Science) according to manufacturer's instruction.

Primer-probe selection and characterization

For promoter A transcripts, the exon 1a sequences of mouse and human were fused with exon 2. For promoter B transcripts, the exon 1b sequences were fused with

exon 2. Forward primer selection was restricted to the exon 1a and exon 1b sequences. The reverse primer selection was restricted to exon 2. In addition, the probe selection was restricted to sequences in exon 1a or 1b or flanking the exon 1 (a or b) and exon 2 splice junction.

The unique sequences for promoter A and B were analyzed using the software, TaqMan® Quantification, to identify suitable primer and probe sets. Mouse and human *Wnt5a* promoter transcript sequences were entered into the software, and the melting temperature and the GC base pair content (for forward, reverse primers and probe) were taken into account during the designing process for each transcript. The primer-probe sets were synthesized by Applied Biosystems, Inc. The selected primer-probe sets are shown in Table 2.

Real time quantitative PCR (qRT-PCR)

For a general qRT-PCR reaction, a 10 μ L reaction was prepared containing TaqMan 1X buffer, primer-probe and cDNA. For most of the qRT-PCR assays, the cDNA samples were first diluted 1:5 in water. Each specific primer-probe and cDNA reaction was run in triplicate from a Master Mix. Essentially, a Master Mix is prepared containing a 29.7 μ L mixture of specific primer-probe and TaqMan 1X buffer and 3.3 μ L of cDNA sample. 10 μ L of this reaction mix is pipetted into 3 individual wells on the reaction plate. qRT-PCR was conducted in StepOne Real Time PCR System thermal

cycling block from Applied Biosystems. The standard amplification condition were 95°C for 15 seconds and 60°C for 1 minute for 40 cycles.

Determination of amplification efficiency

Promoter A and promoter B primer-probes must have similar amplification efficiencies for successful quantification of the specific transcript levels. We determined amplification efficiency by running a five-point dilution series standard curve, using the PCR products previously generated. An initial amplification using standard conditions was run for both mouse and human primer-probe sets to determine product length. The PCR products were then analyzed on a 2% DNA agarose gel to confirm correct product sizes. Confirming the correct product sizes, the PCR product was purified using Qiagen QIAquick PCR purification kit according to the instruction manual. The O.D. values of the purified PCR product were read at 260 and 280 nm and used for determining the concentration.

An initial amplification test was performed using 1 μ L of the purified PCR product in a 10 μ L qRT-PCR reaction to determine the C_T ($\Delta\Delta C_T$) value or cycle number. These cycle numbers then served as a basis for determining the dilution series of the standard curve. A standard curve for PCR product would require a minimum of 5-log dilution series with 5 concentration points. An example of a standard dilution will be 1, 1:10, 1:100, 1:1,000, 1:10,000.

Once the cycle number was known from the initial test, the range for five concentration points were adjusted such that the C_T value was between 10 and 32 cycles with 3.3 cycles per 1:10 dilution. Each concentration consisted of three replicas, resulting in a total of 30 wells (5 dilutions X 3 replicas X 2 promoter targets). The data generated were entered into Microsoft Excel. The 3 replica- C_T values were averaged and used to plot the standard curve.

Each concentration point was plotted on the x-axis, and the averaged C_T value was plotted on the y-axis. Efficiency value was calculated using the equation:

$E = 10^{(-1/\text{slope})} - 1$. According to Applied Biosystems' protocol, efficiency values between 90 and 100% were considered acceptable (Applied Biosystems, 2008).

Analysis of promoter A and promoter B specific transcripts during 3T3-L1 differentiation

The staged 3T3-L1 cells were obtained from Dr. Yashomati Patel's lab (UNCG Biology): *exponential preadipocyte (EX PA)*, *confluent preadipocyte (CON PA)*, *confluent preadipocyte two days after MDI induction (D2 Post MDI)*, and *mature adipocyte (Diff AD)*. RNA was purified from the cells and converted to cDNA as previously described. The cDNA was diluted 1:5 in water and used for qRT-PCR. Primers used for amplification include promoter A and promoter B primer-probe sets, GAPDH (Mm03302249_g1) and ribosomal protein large, PO pseudogene, RPLPOP3 (Mm01974474_gH).

For a single real time PCR reaction composing *EX PA*, *CON PA*, *D2 Post-MDI* and *Diff AD* stages, the following are required: 1) *EX PA* stage's cDNA with promoter A primer (3x replicas), promoter B primer (3x replicas), GAPDH (3xreplicas), ribosomal protein (3x replicas); 2) *CON PA* stage's cDNA with promoter A primer (3x replicas), promoter B primer (3x replicas), GAPDH (3x replicas), ribosomal protein (3x replicas); 3) *D2 Post MDI* stage's cDNA with promoter A primer (3x replicas), promoter B primer (3x replicas), GAPDH (3x replicas), ribosomal protein(3x replicas); and 4) *Diff AD* stage's cDNA with promoter A primer (3x replicas), promoter B primer (3x replicas), GAPDH (3x replicas), ribosomal protein (3x replicas); 5) Promoter A standard 5 dilution points (3x replicas); 6) Promoter B standard 5 dilution points (3x replicas). A total of 78 wells were used for a complete quantification.

C_T values generated from the promoter A and promoter B PCR amplification for the standard curve was graphed in Microsoft Excel to generate a standard curve with transcript numbers on the x-axis and cycle numbers on the y-axis. Transcript numbers were determined using the known mass amount per reaction and molecular weight of the PCR product. A linear equation was generated from the standard curve. The linear equation allowed us to determine the transcript numbers amplified from promoter A and promoter B specific primer-probes by plugging the average C_T number into y.

Analysis of promoter A and promoter B specific transcripts in osteoblast and osteosarcoma

The osteoblasts RNA samples (Catalog C-12720) were purchased from PromoCell. The RNA isolated from the osteosarcoma cells, SaOS-2, and the purchased osteoblasts RNA was converted to cDNA and used for qRT-PCR.

The osteoblasts and osteosarcoma qRT-PCR reactions were set up the same fashion as 3T3-L1 with GAPDH (Hs99999905) as internal control. An assay set comparing osteoblast to SaOS-2 RNA consisted of the following: 1) Promoter A PCR five diluted concentration points (3x replicas); 2) Promoter B PCR five diluted concentration points (3x replicas); 3) Osteoblast cDNA with promoter A primer (3x replicas), promoter B primer (3x replicas), GAPDH (3x replicas); 4) Osteosarcoma cDNA with promoter A primer (3x replicas), promoter B primer (3x replicas), GAPDH (3x replicas). A total of 48 wells were used in a complete quantification. The data were analyzed as for 3T3-L1 cells.

Transient transfection and luciferase assay

Osteosarcoma cancer cells, SaOS-2, were grown to 80% confluency in 24-well plates at 2×10^4 cells per well. Promoter A and promoter B luciferase constructs were individually transfected into SaOS-2 cells along with the *Renilla* control vector (phRL-SV40) using NanoJuice Transfection Kit (Novagen). 0.5 μ L NanoJuiceCore and 0.75 μ L NanoJuice Booster were used per 20 μ L transfection mix. Transfection was performed

according to the manufacturer's protocol. 24-48 hours after transfection, cells were collected. The medium was removed from each well and 500 μ L of PBS was added and removed to wash the cells. 150 μ L of Passive Lysis Buffer (Promega, Inc) was added to each well and the plate was incubated at room temperature on a shaker. The cell lysate were assayed for firefly and *Renilla* luciferase activity utilizing the Dual-Luciferase Reporter assay system (Promega, Inc). 20 -30 μ L samples from each well were transferred to a 96 well black-welled plate. The samples were assayed for firefly and *Renilla* luciferase activity on a Synergy 2 multimode microplate reader (BioTek).

CHAPTER III

RESULTS

Custom design primer and probe sets

To amplify the specific transcripts generated by *Wnt5a* alternative promoter A and promoter B in both human and mouse, TaqMan primer-probe sets for qRT-PCR were custom designed in conjunction with a previous lab member (Joyner-Powell, N). The primer-probe sets were designed according to the approach described in the Materials and Methods section. The forward primers for both promoter transcripts were located within the unique exon sequence 1a and 1b (Figure 1). The sequences of the forward and reverse primer and probes are shown in Table 2. The probe sequences are homologous to sequences either in exon 1 (a or b) plus exon 2, the first and second exons thus flanking the splice junction, for the primer-probe sets for mouse promoter A, human promoter A and human promoter B. The probe sequence for mouse promoter B is located in exon 2. The locations of primer and probe sequences within the cDNA sequences are shown in Figure 2.

The primer-probe sets were initially tested to confirm the correct sizes of the promoter A and promoter B PCR products. The PCR products generated from the qRT-PCR reactions were run on a 2% DNA agarose gel (Figure 3A and B). These results

confirmed that both human and mouse custom designed primers-probes amplified qRT-PCR products of the expected size.

Figure 2. Location of mouse and human primer-probe sets in exon 1 (a or b) plus cDNA sequences. Forward primer sequence is shown in red. Reverse primer sequence is shown in blue. Probe sequence is shown in Green. Asterisk * indicates the splice junction between exons. **A.** Mouse promoter A cDNA. **B.** Mouse promoter B cDNA. **C.** Human promoter A cDNA. **D.** Human promoter B cDNA.

A.

```

                                Forward                                Probe
                                20                                40                                50
10                                30                                40                                50
CTTCGCTCGG GTGGCGACTT CCTCTCCGTG CCCCCTCCCC CTCGCCATGA
GAAGCGAGCC CACCGCTGAA GGAGAGGCAC GGGGGAGGGG GAGCGGTACT

*      60      70      80      90      100
AGAAGCCCAT TGGAATATTA AGCCCGGGAG TGGCTTTGGG GACCGCTGGA
TCTTCGGGTA ACCTTATAAT TCGGGCCCTC ACCGAAACCC CTGGCGACCT
                                Reverse

110      120      130      140      150
GGTGCCATGT CTTCCAAGTT CTTCCTAATG GCTTTGGCCA CGTTTTTCTC
CCACGGTACA GAAGGTTCAA GAAGGATTAC CGAAACCGGT GCAAAAAGAG

160      170      180
CTTCGCCCAG GTTGTTATAG AAGCTAATTC TTGGTG
GAAGCGGGTC CAACAATATC TTCGGTTAAG AACCAC

```

B.

```

                                Forward                                *                                Probe
                                20                                30                                40                                50
10                                20                                30                                40                                50
ACTTGTGCT CCGGCCCAGA AGCCATTGG AATATTAAGC CCGGGAGTGG
TGAACAACGA GGCCGGGTCT TCGGGTAACC TTATAATTCTG GGCCCTCACC
                                Reverse

60      70      80      90      100
CTTTGGGGAC CGCTGGAGGT GCCATGTCTT CCAAGTTCTT CCTAATGGCT
GAAACCCCTG GCGACCTCCA CGGTACAGAA GGTTCAAGAA GGATTACCGA

110      120      130      140      150
TTGGCCACGT TTTTCTCCTT CGCCAGGTT GTTATAGAAG CTAATTCTTG
AACCGGTGCA AAAAGAGGAA GCGGGTCCAA CAATATCTTC GATTAAGAAC

GTG
CAC

```

C.

Forward

260 270 280 290 300
TCCGCTCGGA TTCCTCGGCT GCGCTCGCTC GGGTGGCGAC TTCCTCCCCG
AGGCGAGCCT AAGGAGCCGA CGCGAGCGAG CCCACCGCTG AAGGAGGGGC

Probe

310 320 * 330 340 350
CGCCCCCTCC CCCTCGCCAT GAAGAAGTCC ATTGGAATAT TAAGCCCAGG
GCGGGGGAGG GGGAGCGGTA CTTCTTCAGG TAACCTTATA ATTCGGGTCC

Reverse

360 370 380 390 400
AGTTGCTTTG GGGATGGCTG GAAGTGCAAT GTCTTCCAAG TTCTTCCTAG
TCAACGAAAC CCCTACCGAC CTTACAGTTA CAGAAGGTTC AAGAAGGATC

D.

Forward

10 20 30 40 *

CTCCTCTCGC CCATGGAATT AATTCTGGCT CCACTTGTTG CTCGGCCCAG
GAGGAGAGCG GGTACCTTAA TTAAGACCGA GGTGAACAAC GAGCCGGGTC

Reverse

60 70 80 90 100
AAGTCCATTG GAATATTAAG CCCAGGAGTT GCTTTGGGGA TGGCTGGAAG
 TTCAGGTAAC CTTATAATTC GGGTCCTCAA CGAAACCCCT ACCGACCTTC

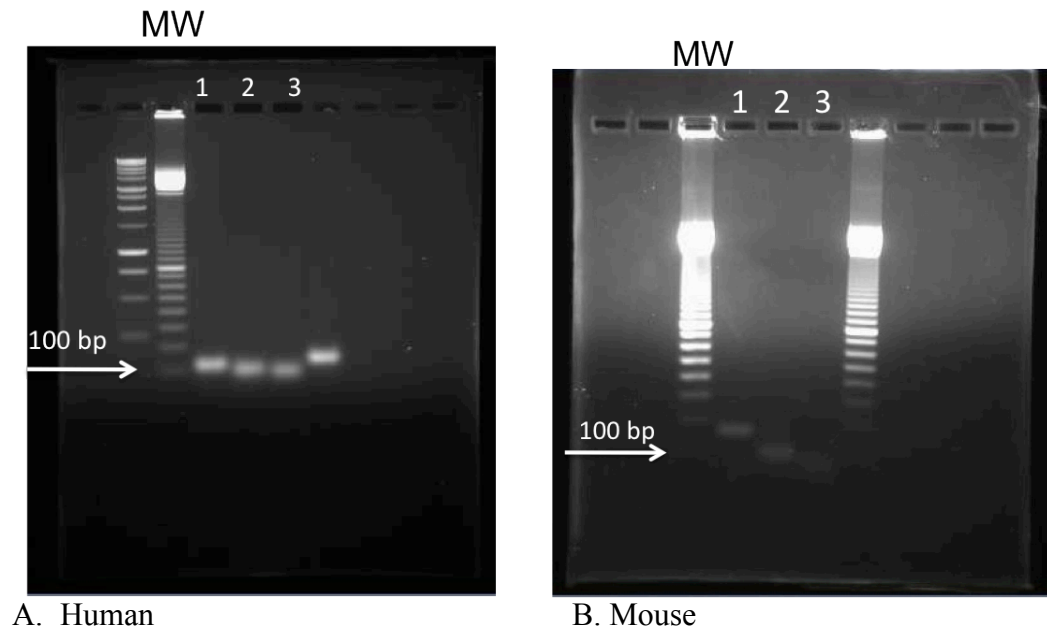
110 120 130 140 150
TGCAATGTCT TCCAAGTTCT TCCTAGTGGC TTTGGCCATA TTTTTCTCCT
ACGTTACAGA AGGTTCAAGA AGGATCACCG AAACCGGTAT AAAAAAGAGGA

160 170 180
TCGCCCAGGT TGTAATTGAA GCCAATTCTT GGTG
AGCGGGTCCA ACATTAACTT CGGTTAAGAA CCAC

Table 2. *Wnt5a* custom designed mouse and human primer-probe sets

	Sequence (5' → 3')	Length (base)	Product Size (bp)
Mouse Promoter A			
Forward	GTGGCGACTTCCTCTCCGT	19	85
Reverse	AGTGGCTTTGGGGACCG	17	
Probe	CCCCTCGCCATGAAGAAGCCCA	22	
Mouse Promoter B			
Forward	ACTTGTTGCTCCGGCCC	17	62
Reverse	CGGTCCCCAAAGCCACT	17	
Probe	AGAAGCCCATTGGAATATTAAGCCCGG	27	
Human Promoter A			
Forward	TCGGGTGGCGACTTCCT	17	77
Reverse	TAACCTTATAATTCGGGTCCTCAAC	25	
Probe	CGCCCCCTCCCCCTCGCCATGAAG	24	
Human Promoter B			
Forward	CCTCTCGCCCATGGAATT	18	71
Reverse	CTTCAGGTAACCTTATAATTCGGG	24	
Probe	CTGGCTCCACTTGTTGCTCGGCC	23	

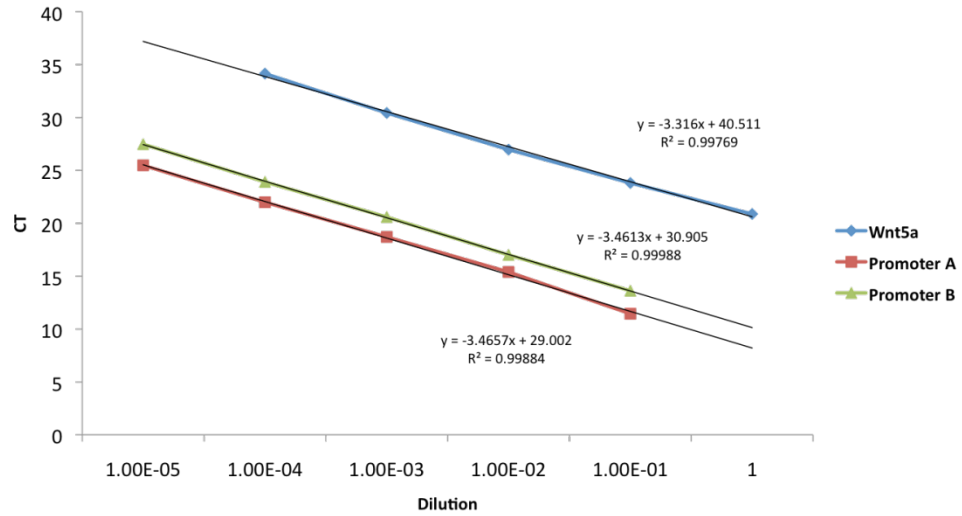
Figure 3. Wnt5a qRT-PCR product sizes. **A. Human primer-probe sets.** Lane 1– Applied Biosystems primer-probe for Wnt5a detects both promoter A and promoter B transcripts, 101bp. Lane 2 – Promoter A primer-probe set, 77bp. Lane 3 – Promoter B primer-probe set, 71bp. **B. Mouse primer-probe sets.** Lane 1 – Applied Biosystems primer-probe set for Wnt5a, 158bp. Lane 2 – Promoter A primer-probe set, 85bp. Lane 3 - Promoter B primer-probe set, 62bp. MW – 100 bp molecular weight marker.



For successful quantification of transcript levels, promoter A and promoter B primer-probes must have similar amplification efficiencies. We determined amplification efficiency by running a four or five-point dilution series standard curve, using the PCR products previously generated (Figure 3A and B). The standard curve generated from this reaction (Figure 4A and B) allowed us to calculate the efficiency value of the primers by using the equation, $E = 10^{(-1/\text{slope})} - 1$. We obtained efficiency values of 94.5% for promoter A and 94.3% for promoter B from human custom designed primer-probe sets (Table 3). The mouse custom designed primers showed efficiency values of 99.5% for promoter A and 92% for promoter B. These amplification efficiency values are within the range of $90 - 100 \pm 10\%$, indicating that our custom designed primer-probe sets are suitable for further experimentation (Applied Biosystems, 2008).

Figure 4. Custom designed *Wnt5a* primer-probe efficiency curves. Purified PCR products generated from qRT-PCR amplification (Figure 2) were diluted from 10^1 to 10^4 or 10^5 and amplified using the human (A) and mouse (B) specific primer-probe sets for promoter A and promoter B. The Applied Biosystems primer-probe for *Wnt5a* is also shown.

A.



B.

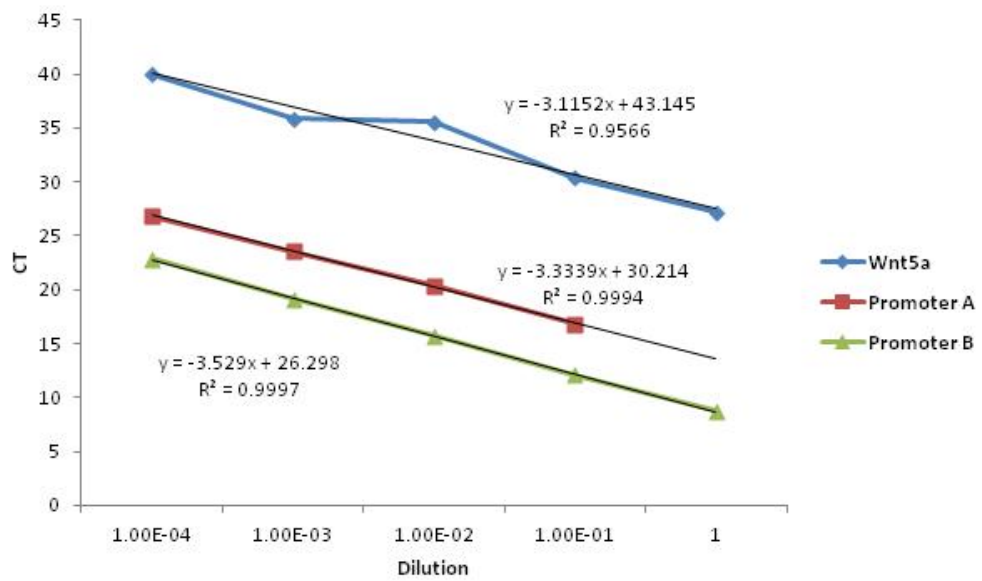


Table 3. *Wnt5a* custom designed primer-probe amplification efficiency values

	Human	Mouse
Promoter A	94.5 ±10 %	99.50 ±10 %
Promoter B	94.3 ±10 %	92.0 ±10 %

Mouse Wnt5a promoter A and promoter B transcript levels during differentiation of 3T3-L1 cells

The levels of promoter A and promoter B generated transcripts were analyzed during cellular differentiation of 3T3-L1 mouse fibroblasts into adipocytes. 3T3-L1 cells at different periods of differentiation were obtained from Dr. Yashomati Patel's lab from UNCG Biology Department. These are referred to as Set 1. The second set, Set 2, was RNA isolated from 3T3-L1 cells at different periods of differentiation, and they were obtained from Dr. Ron Morrison's lab from the UNCG Nutrition Department. These RNA samples were converted to cDNA.

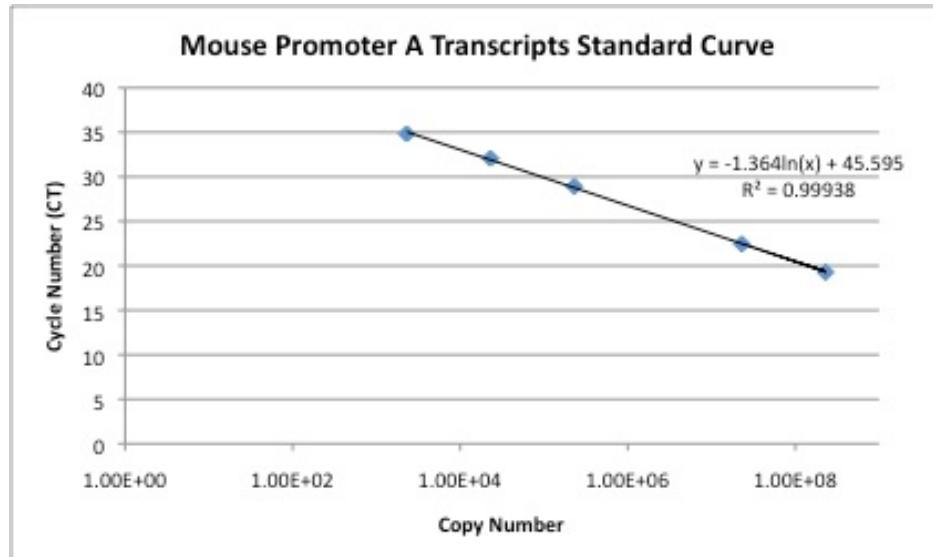
In the Set 1 experiment, 1 µg of RNA extracted from the cells was utilized per cDNA synthesis reaction. The amplification reaction was 20 µL and the cDNA was diluted 1:5. Hence, each qRT-PCR reaction contained the equivalent of 0.01 µg of RNA. The PCR cycle numbers generated from a five-point dilution series for promoter A and promoter B were used to generate the standard curve with known molecule numbers of PCR template on the x-axis and cycle numbers (C_T) on the y-axis (Figure 4). The standard curve equation allows us to calculate the absolute copy numbers of the promoter A and promoter B specific transcripts generated from the PCR reaction (Table 4).

The transcript copy numbers are compared in the graph shown in Figure 6A and B. Set 1 Promoter A transcripts increased in the confluent cell stage (CON PA) in comparison to exponential preadipocytes (EX PA), decreased in the cell stage two days after MDI treatment (D2 Post-MDI) and increased again in the differentiated adipocytes stage (Diff AD).

Promoter B transcript levels in Set 1 were similar in exponential (EX PA) and confluent (CON PA) preadipocytes (Figure 6B). Promoter B transcripts decreased two days after MDI treatment (D2 Post-MDI), and remained low in differentiated adipocytes (Diff AD). The ratios of promoter A to promoter B transcripts at the different stages of cellular differentiation were determined (Figure 7). In exponential preadipocytes (EX PA), there was approximately 10-fold more promoter A transcripts than promoter B transcripts. The ratio of A to B transcripts continued to increase at each stage. In the differentiated adipocytes (Diff AD), there were approximately 120-fold more promoter A transcripts than promoter B.

Figure 5. Mouse *Wnt5a* promoter A and promoter B PCR standard curves. A. Promoter A specific transcript PCR standard curve. **B.** Promoter B specific transcript PCR standard curve. X-axis is the absolute copy number of the PCR product in the reaction and y-axis is the cycle number.

A.



B.

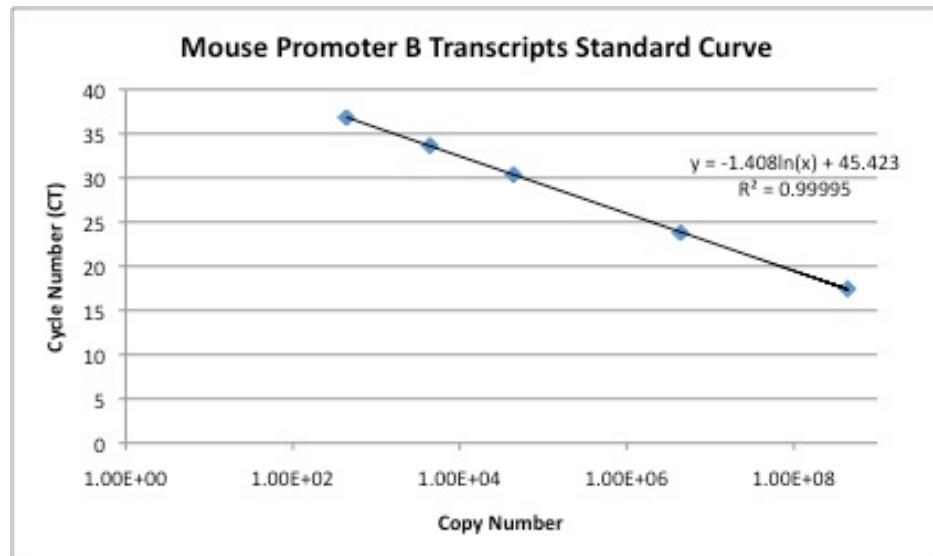


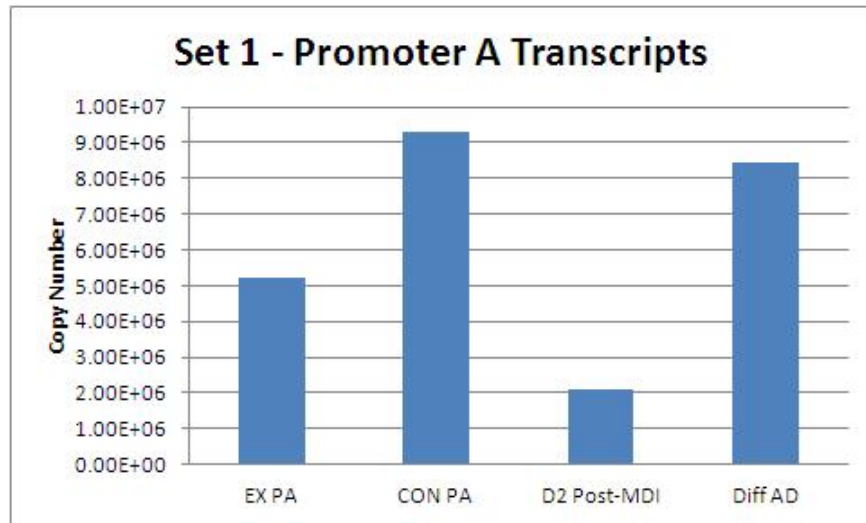
Table 4. Comparison of 3T3-L1 Set 1 and Set 2 transcript levels. Numbers represent number of transcripts per 0.01 μ g of RNA

	EX PA ¹	CON PA ²	D1 Post MDI ³	D2 Post MDI ³	Diff. AD ⁴
Set 1 Promoter A	5.20E+06	9.31E+06	—	2.10E+06	8.42E+06
Set 1 Promoter B	4.11E+05	4.20E+05	—	5.21E+04	6.65E+04
Set 2 Promoter A	—	3.76E+06	8.47E+05	1.05E+06	2.85E+06
Set 2 Promoter B	—	1.37E+06	2.03E+05	1.86E+05	1.82E+05

1. Exponentially growing preadipocytes (3T3-L1)
2. Confluent preadipocytes (3T3-L1)
3. One day (D1) and two days (D2) after MDI treatment
4. Differentiated adipocytes

Figure 6. Promoter A and Promoter B transcript levels during the course of 3T3-L1 cellular differentiation, from preadipocytes to adipocytes. Set 1 RNA samples: Exponentially growing preadipocytes (EX PA), Confluent preadipocytes (CON PA), Two days after MDI treatment (D2 Post-MDI), and Differentiated Adipocytes (Diff AD).

A.



B.

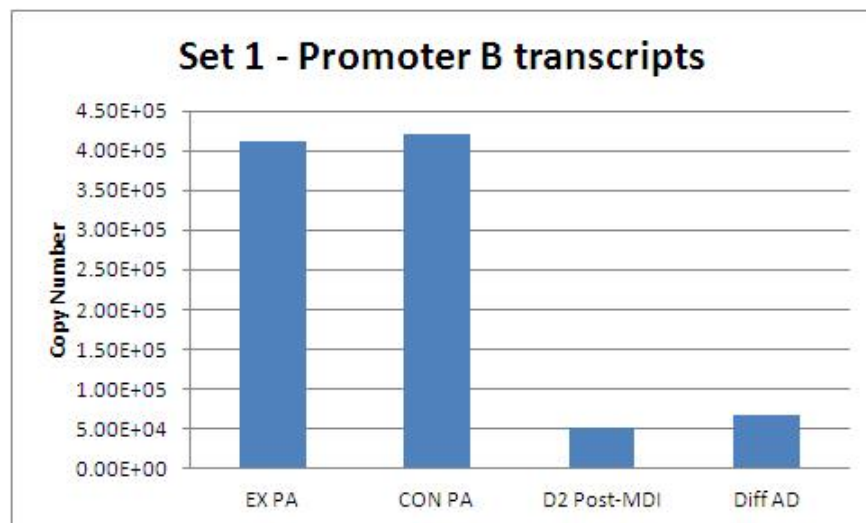
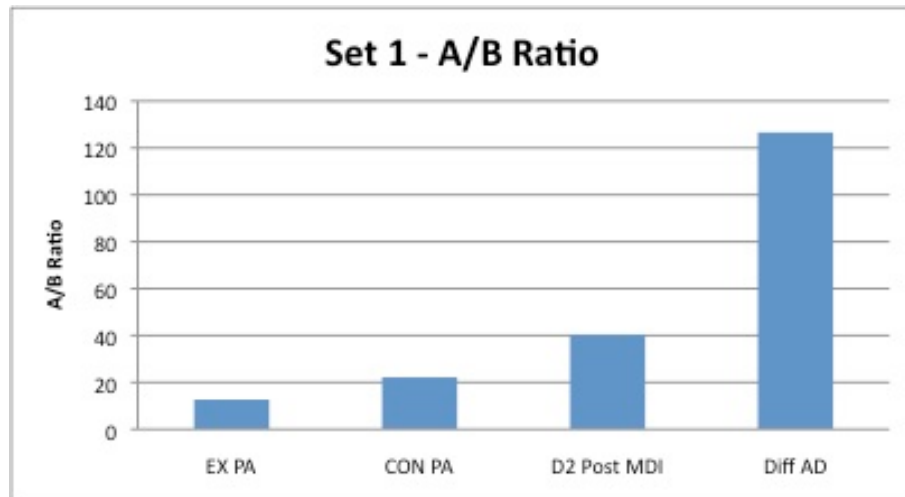


Figure 7. Mouse *Wnt5a* promoter A to promoter B transcript number ratios during differentiation of 3T3-L1 cells. The transcript numbers in Table 4 were used to determine the A/B ratio at each stage.



To confirm the results from Set 1, we used RNA graciously provided by Dr. Ron Morrison (UNCG, Department of Nutrition). These RNA samples were derived from confluent preadipocytes (CON PA), one day after MDI treatment (D1 Post MDI), two days after MDI treatment (D2 Post MDI) and differentiated adipocytes (Diff AD).

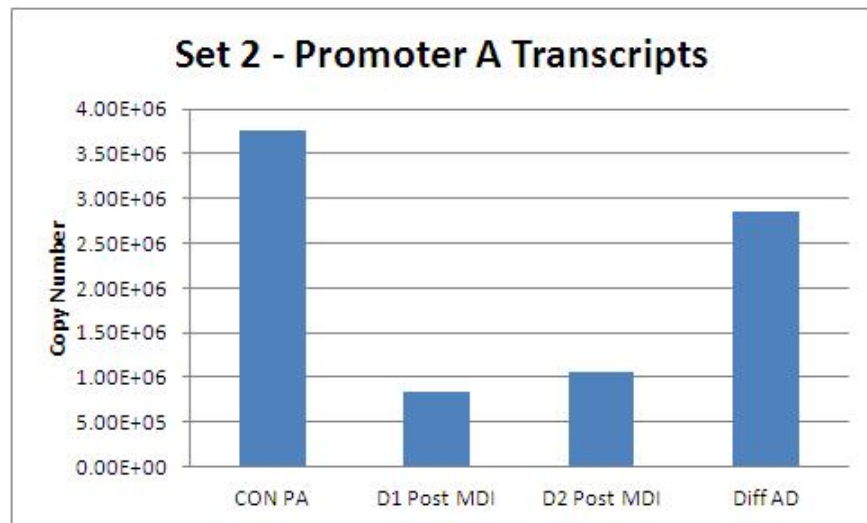
Promoter A specific transcripts generated from Set 2 showed similar changes in levels during the course of cellular differentiation as in Set 1. A decrease level in transcripts was measured after MDI induction (D1 and D2 Post MDI), and an increase of transcript numbers in mature differentiated adipocytes (Diff AD) (Figure 8A).

After MDI induction, the level of promoter B transcripts decreased significantly and remained at the same low level in the mature adipocytes (Diff AD) (Figure 8B). The ratio of promoter A to promoter B transcripts numbers during different stages of 3T3-L1

differentiation was similar to Set 1 in that the ratio increased from preadipocytes to mature adipocytes. However, the ratio values were approximately 10-fold less. This was due to there being approximately 10X more promoter B transcripts and the lower level of promoter A transcripts in Set 2 than Set 1 (See Figures 7 and 9).

Figure 8. Transcript numbers in 0.01 μ g of RNA derived from *Wnt5a* promoter A and promoter B during the course of 3T3-L1 differentiation, Set 2. Set 2 RNA samples: Confluent preadipocytes (CON PA), One day after MDI treatment (D1 Post-MDI), Two days after MDI treatment (D2 Post-MDI) and Differentiated Adipocytes (Diff AD).

A.



B.

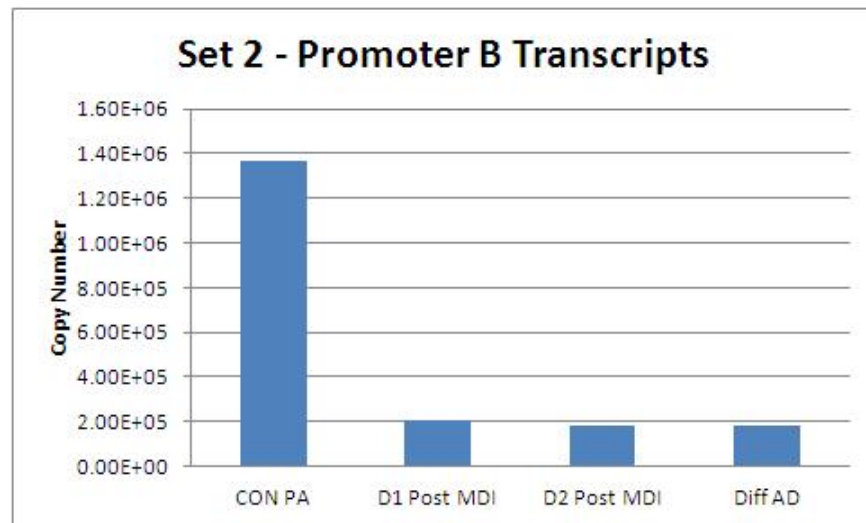
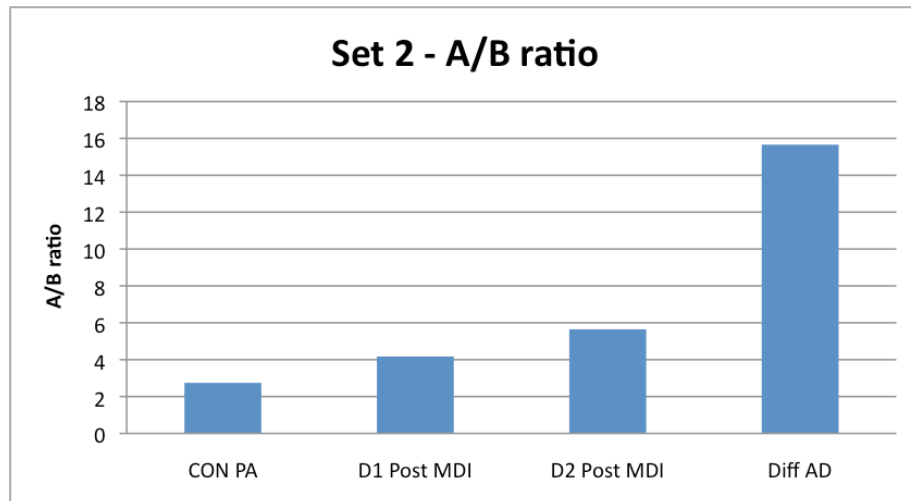


Figure 9. Mouse *Wnt5a* promoter A to promoter B transcript number ratios in 3T3-L1. The transcript numbers in Table 4 were used to determine the A/B ratio at each stage.



Human Wnt5a alternative promoter A and promoter B transcript levels in osteoblasts and osteosarcoma cells

Human *Wnt5a* promoter A and promoter B transcripts were quantified using the same procedure as for the 3T3-L1 cells. 1 µg of RNA extracted from the osteosarcoma cells and osteoblasts were utilized per cDNA synthesis reaction and for the qRT-PCR reaction. The qRT-PCR cycle numbers generated from a five-point dilution series for promoter A and promoter B specific PCR products were used to generate the standard curve (Figure 10 A and B) with known molecule numbers on the x-axis and cycle numbers on the y-axis. The standard curve equation allowed us to calculate the absolute

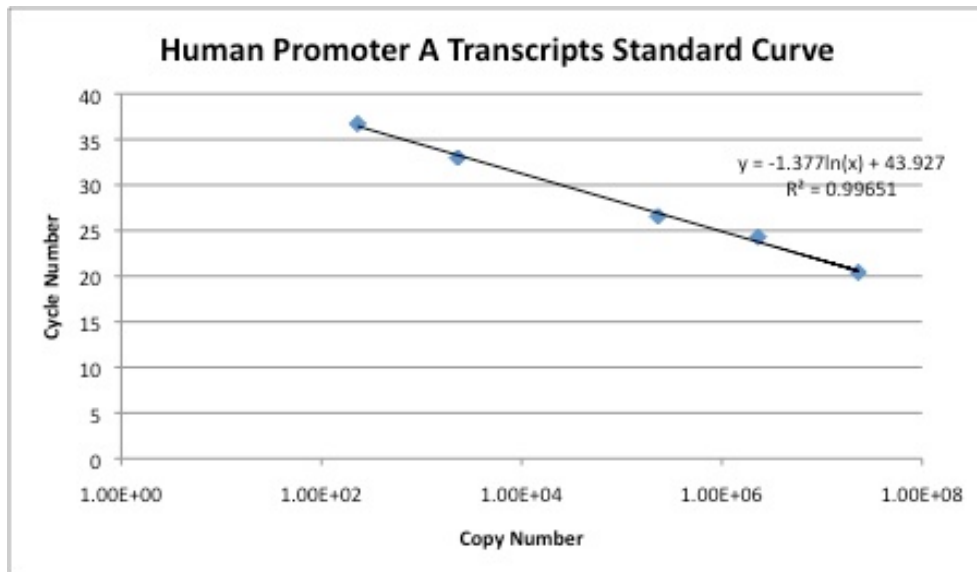
copy numbers of the promoter A and promoter B specific transcripts generated from the qRT-PCR reactions (Figure 8A and B; Table 6).

In osteoblasts cells, the level of promoter A and promoter B transcripts are nearly equivalent (6.5×10^5 versus 4.4×10^5) (Figure 12; Table 5). In contrast, there are nearly 2.33×10^3 more promoter A than promoter B transcripts in osteosarcoma cells (Figure 11 B; Table 5). In fact, promoter B transcripts were nearly undetectable by qRT-PCR.

The ratio of promoter A to promoter B transcript numbers in osteoblast and osteosarcoma cells is shown in Figure 12. In osteoblasts, the ratio is nearly 1, whereas in osteosarcoma cells, the ratio is 2320:1.

Figure 10. Human *Wnt5a* specific promoter A and promoter B PCR standard curve.
A. Promoter A specific transcripts PCR standard curve. **B.** Promoter B specific transcript PCR standard curve. X-axis is the absolute copy number of the PCR product in the reaction and y-axis is the cycle number.

A.



B.

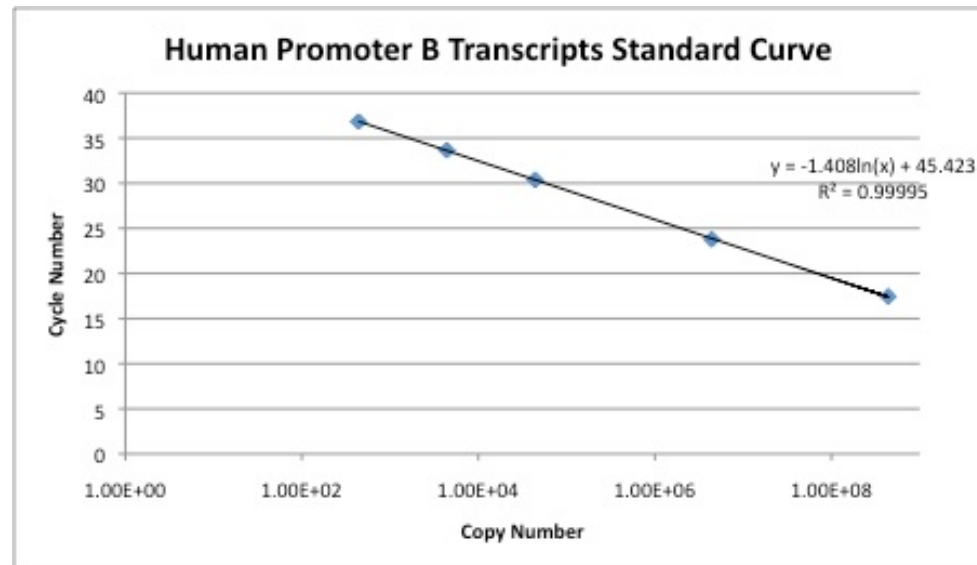
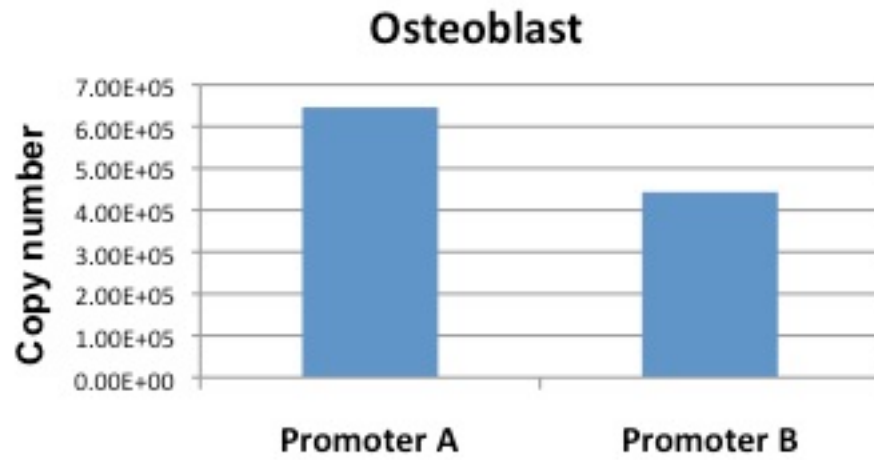


Figure 11. Numbers of *Wnt5a* promoter A and promoter B specific transcripts in osteoblasts and osteosarcoma RNA. Number of *Wnt5a* promoter A and promoter B specific transcripts per 0.25 μ g RNA.

A.



B.

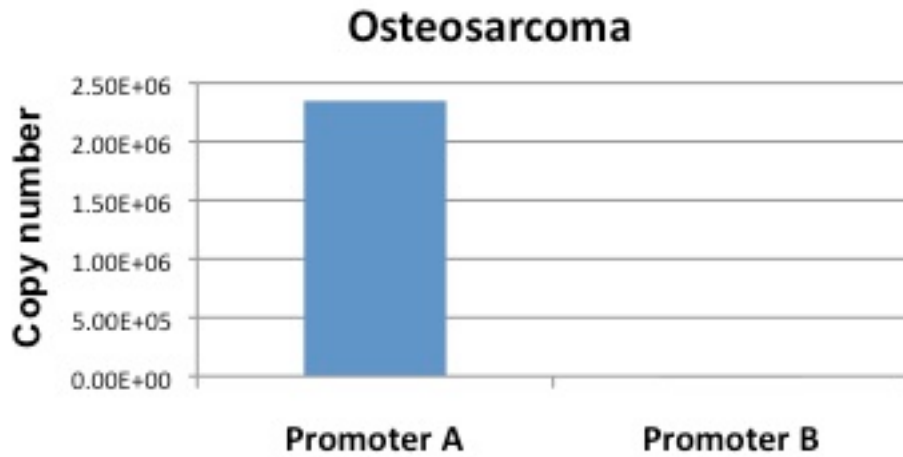
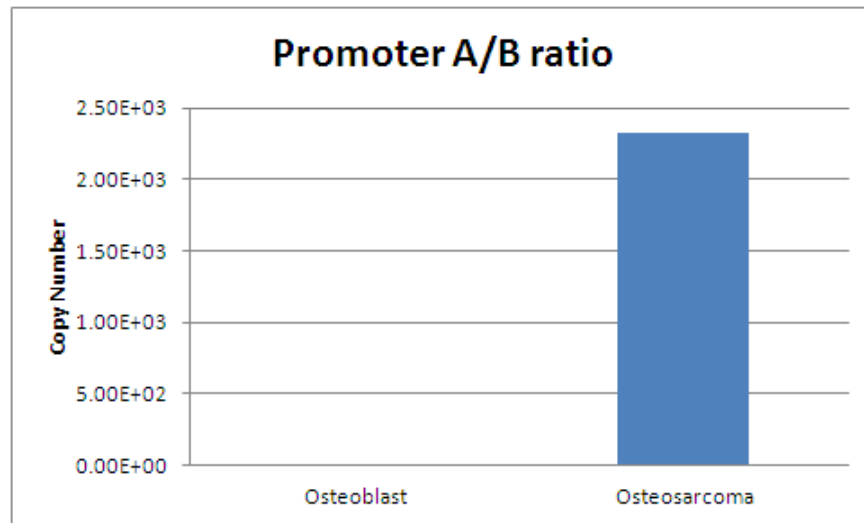


Table 5. *Wnt5a* promoter A and promoter B specific transcripts in 0.25 µg of osteoblast and osteosarcoma RNA.

	Osteoblast	Osteosarcoma
Promoter A	6.46E+05	2.35E+06
Promoter B	4.43E+05	1.01E+03
A/B ratio	1.46E+01	2.32E+03

Figure 12. Ratio of *Wnt5a* promoter A to promoter B transcripts in osteoblast and osteosarcoma RNA. The transcript numbers in Table 5 were used to determine the A/B ratio.



Activity of separated promoter A and promoter B in osteosarcoma cells

Luciferase reporter constructs containing different lengths of human promoter A and promoter B upstream sequences were constructed (Katula *et al.* 2012, submitted) (Figure 13). These reporter constructs were transfected into osteosarcoma cells, SaOS-2, along with the *Renilla* control vector, and the promoter activities were expressed as Firefly/*Renilla* relative light units.

After 48 hours, the cell lysates were collected and assayed for firefly and *Renilla* luciferase activity and the ratio of Firefly/*Renilla* determined. For promoter A constructs, activity levels varied 2-4 fold. The reduction in activity for constructs p1358 and p773 suggests a loss of positive acting sequences between 1707 and 1358 base pairs. The increase between p773 and p420 indicates the loss of negative acting sequence in this sequence region. The promoter B constructs expressed at a similar level, indicating the sequences for maximum expressions are located within the first 356 base pairs, although it is possible that there are negative acting sequences between 1981 and 1257 base pair. Most importantly, the level of expression from promoter A and promoter B are nearly equal. This indicates that the lack of promoter B transcripts in osteosarcoma cells (Figure 12B) is not due to a reduction in promoter B specific transcription factors.

Figure 13. *Wnt5a* human promoter A and promoter B luciferase reporter constructs (Katula *et al.* 2012 submitted). The numbers are base pair upstream from the first nucleotide of the cDNA indicated with the NCBI accession number and is represented by the black line. The boxes are sequences downstream of the first nucleotide. The indicated *Hind* III and *Bgl* III sites were used for cloning. The scale bar applies only to the *Wnt5a* sequences and not the vector. The promoter B construct includes a 41 base pair intron, unique to the promoter B transcripts.

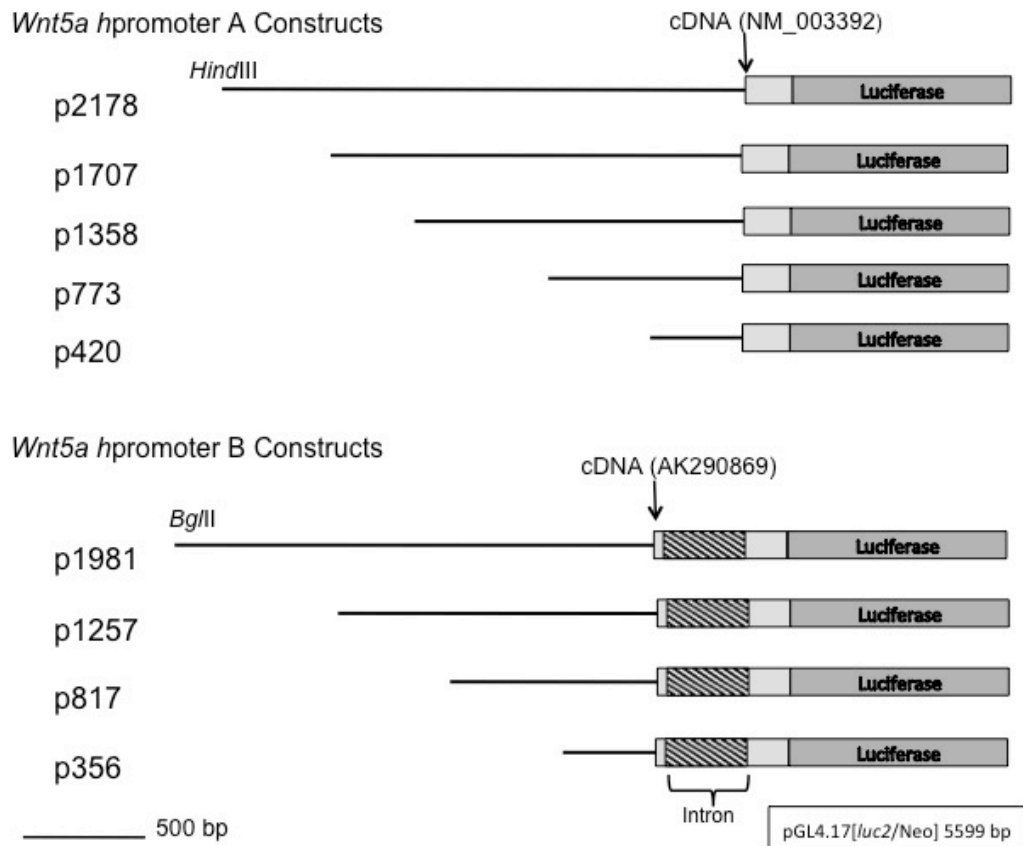
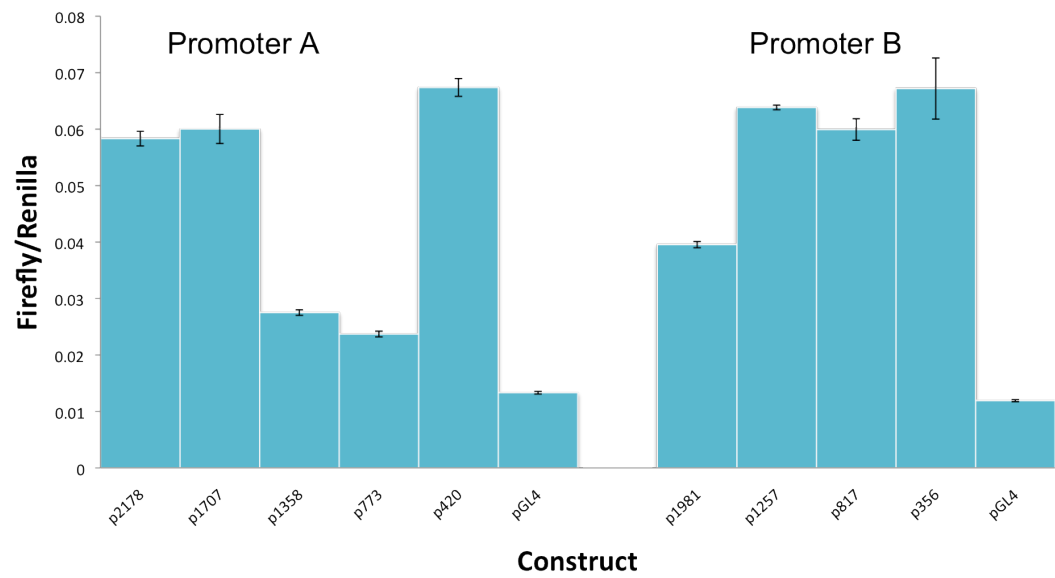


Figure 14. Relative activity levels of human *Wnt5a* promoter A and promoter B deletion constructs in osteosarcoma, SaOS-2 cells. Each of the constructs shown in Figure 11 were transfected into SaOS-2 cells. pGL4 is the reporter vector without any insert. The levels of *Renilla* and firefly luciferase activity were determined and promoter activity expressed as the ratio of firefly to *Renilla* relative light units. The bars are +/- S.E.M.



CHAPTER IV

DISCUSSION

Overview

WNT5a is a secreted glycoprotein that has been shown to be involved in cellular development, differentiation and homeostasis. The *Wnt5a* gene generates multiple transcripts through alternative splicing and different transcription start sites. These transcripts generate different protein isoforms, which are likely to have distinct functions. Previous studies have shown that *Wnt5a* expression is often misregulated during cancer progression and increases in metastasizing cancer cells (Silver *et al.* 2009). However, the molecular mechanisms underlying *Wnt5a* altered expression are not well understood. Also, nothing is known regarding the utilization of the *Wnt5a* alternative promoters during cellular development. In this study, we examined the transcripts derived from *Wnt5a* transcription start sites termed promoter A and promoter B during cellular differentiation by measuring the specific transcripts in different stages of 3T3-L1 mouse fibroblasts as they differentiate into adipocytes. We also measured the specific transcript levels during cancer progression using normal human osteoblasts and osteosarcoma cells as a model. In general, our results suggest that the *Wnt5a* alternative promoters A and B are differentially regulated. We found that promoter A is expressed at a higher level than

promoter B and that promoter B transcript levels vary to a greater degree than promoter A transcripts.

Custom designed primer-probe sets for Wnt5a alternative promoter A and promoter B

To amplify specific transcripts derived from promoter A and promoter B, we designed TaqMan primer-probe sets for both mouse and human. Since promoter A and promoter B transcripts share the same exon 2, 3, 4, and 5 sequences, the forward primers were designed within the unique exon 1a and 1b sequences to amplify target transcripts. The unique exon 1b in promoter B sequence is relatively short, 47 bp in human and 52 bp in mouse. However, TaqMan primer sets contain a probe that adds specificity in the detection process. This probe contains the fluorescent tag and must hybridize to its specific sequence before a signal can be detected by the instrument. After the probe is annealed to the target sequence, the dye on the probe is removed by the Taq DNA polymerase, allowing it to generate fluorescent signals. Hence, even if the forward and reverse primers amplified a nonspecific genomic sequence, these would not be detected by the instrument, as the probe would only bind to the correct PCR product. Also, the PCR products generated from the reaction were run on a 2% DNA agarose gel, and the results confirmed that our custom designed primer-probe sets were specific and amplified the correct fragment sizes (Figure 2). As such, we are confident that our custom designed TaqMan primer-probe sets are detecting promoter A and promoter B transcripts.

For a direct comparison of transcript molecules in a given sample it was necessary to confirm that the primer-probe sets had the required amplification efficiencies. We determined the efficiency of the custom designed primer-probe sets by running a five point dilution standard curve (Applied Biosystems). According to Applied Biosystems, amplification efficiency values between 90 and 100 \pm 10% are considered efficient. Our results showed that the human promoter A and promoter B primer-probe sets have nearly equal efficiency values of 94% (Table 3). For mouse promoter A, the primer-probe set has a higher efficiency value of 99% than the 92.5% from promoter B, but both values are still within the range of acceptable efficiency values. These results confirmed that both mouse and human promoter A and promoter B primer-probe sets are suitable for comparative studies.

Promoter A and promoter B are differentially regulated during 3T3-L1 differentiation

As mentioned in the background, *Wnt5a* has been shown to be expressed in both preadipocytes and mature adipocytes (Imagawa *et al.* 2008). Although total *Wnt5a* levels were examined, nothing has been published regarding the transcripts derived from the *Wnt5a* alternative promoters. In this study, we determined the level of *Wnt5a* alternative promoters A and B transcripts during adipocyte differentiation.

Our data indicate that promoter A and promoter B are differentially regulated during adipocyte differentiation. Promoter A transcript levels increased in exponential preadipocytes and confluent preadipocytes, but decreased two days after MDI treatment

and increased in differentiated adipocytes. In contrast, promoter B transcript levels increased in exponential preadipocytes and confluent preadipocytes, decreased two days after MDI treatment and remained at a low level in differentiated adipocytes.

We determined the ratio of A to B transcripts and found that the proportion of A transcripts increased continually. In mature adipocytes, there were nearly 120X more A transcripts than B, whereas, in growing preadipocytes, there were 10X more A transcripts than B. These data suggest that the promoter A derived protein isoforms play a greater role in mature adipocytes and that both A and B protein isoforms have functions in growing adipocytes. However, this is only speculative as it is not known if the levels of protein isoforms correspond to the mRNA levels.

It is not clear why the determined levels of promoter B transcripts were nearly 10 fold higher in Set 2 than Set 1 and that promoter A transcripts were 2 to 3 fold lower. Together, this leads to smaller differences between A and B in Set 2. For example, the A/B ratio in Set 2 was 2X and 16X in confluent and in mature adipocytes respectively, whereas for Set 1, it was 10X and 120X. It is possible that these differences are due to the uniqueness of the cell lines, as the two labs obtained their 3T3-L1 cells from a different source. In addition, there is the possibility that the levels of *Wnt5a* methylation differ in each cell line due to different periods of cell growth. For example, the lower level of promoter B expression in the 3T3-L1 cells from Dr. Patel's lab could be due to more DNA methylation in the promoter B associated CpG islands. Nevertheless, the ratio of A/B from both sets showed a similar pattern of transcript levels, in which both

promoter A and promoter B transcript levels decreased after MDI treatment and promoter A transcripts increased in mature adipocytes while promoter B transcripts were at a very low level.

Wnt5a alternative promoter A and B are differentially regulated in osteoblast and osteosarcoma cells

We examined the level of promoter A and promoter B transcripts in normal human osteoblasts and the human osteosarcoma cell line, SaOS-2, as a model for cancer progression. While *Wnt5a* expression has been shown to be altered in many cancers (Silver *et al.* 2009), the utilization of the alternative promoters during cancer progression has not been investigated. Our results indicated that *Wnt5a* alternative promoter A and promoter B transcript levels are nearly equal in osteoblasts cells. The similar level of promoter A and promoter B transcripts in osteoblast gives the transcript A/B ratio of 1.46 to 1. In contrast, promoter B transcripts showed a dramatic decrease in osteosarcoma, giving a higher transcript A/B ratio of 2320 to 1. This result suggests that the increase level of promoter A transcripts has functional importance during cancer progression, whereas the promoter B transcripts were nearly diminished in osteosarcoma cells. These results are consistent with other findings, where total *Wnt5a* are constitutively expressed in the osteosarcoma cancer cells, SaOS-2 (Enomoto *et al* 2009).

Decrease in promoter B transcript levels in osteosarcoma cells is unlikely due to changes in transcription factors

In the osteoblast and osteosarcoma qRT-PCR experiment, both promoter A and promoter B are expressed at the same level in normal human osteoblasts RNA, with A/B ratio close to one. In contrast, in osteosarcoma cells, promoter B transcript levels decreased significantly, resulting in a 1600 fold increase in the A/B ratio. One explanation for the decrease in promoter B transcript level is that transcription factors specific to promoter B sequences are reduced in osteosarcoma cells. However, based on our results, this explanation is unlikely. We transfected the osteosarcoma cells, SaOs-2, with luciferase reporter constructs containing different amounts of promoter A and promoter B sequences and found there is no significant difference between the expression level of promoter A and promoter B. If there was a decrease in promoter B specific transcription factors in osteosarcoma cells, the expression level of promoter B constructs should be reduced relative to expression from the promoter A constructs. Therefore, our results suggest the decreased level of promoter B transcripts is not due to reduced transcription factors. An alternative explanation is that promoter B sequences are being epigenetically modified such as DNA methylation. In fact, the DNA sequences associated with the Wnt5a promoter A have been shown to be subjected to methylation from DNA (Wang *et al.* 2007). There are five putative CpG islands in the promoter B upstream sequence regions, and our lab is currently analyzing methylation activities in the promoter B region.

Functional importance of the Wnt5a alternative promoters

In general, our results suggest that the *Wnt5a* alternative promoters A and B are functionally important. First, both human and mouse have conserved promoter A and B transcription start sites. Second, both promoters were found to be active in two different cell types, fibroblasts and osteoblasts. Third, the level of transcripts from promoters A and B vary.

As previously discussed, alternative promoters are common in the human genome and provide for diverse gene regulatory patterns at different developmental stages, in different cell types and under different environmental conditions. *Wnt5a* is involved in a variety of developmental events such as tissue homeostasis and cell differentiation. Thus, our results showing differential expression of the *Wnt5a* alternative promoters are not unexpected.

The mechanisms by which the *Wnt5a* alternative promoters are regulated are not known. Our results suggest that epigenetic regulation may play a role. It is interesting to note that DNA methylation status of alternative promoters of the same gene may differ (Cheong *et al.* 2006). CpG islands are associated with both *Wnt5a* promoter A and promoter B upstream sequences, which could contribute to the differential regulation of the promoters. Our lab is currently analyzing DNA methylation of the CpG-islands in the promoter B region.

It is known that the transcripts generated from *Wnt5a* gene produces different protein isoforms. However, little is known regarding the distinct functions of these

protein isoforms. The transcripts derived from promoter A and promoters B are known to give rise to distinct protein isoforms (see Table 1). In this study, we did not address the question of whether variations in promoters A and B transcript levels correlate with changes in protein levels. Regardless, it is critical to address this question and to examine unique function of the *Wnt5a* protein isoforms.

REFERENCES

1. Andersson E., Prakas N., Cajanek L., Minina E., Bryia V., Bryiova L., Yamaguchii T., Hall A., Wurst W. and Arenas E. 2008. Wnt5a regulates ventral midbrain morphogenesis and the development of A9-A10 dopaminergic cells in vivo. *PLoS One*. Vol 3. Issue 10.
2. Azharuddin S., Leszek H., Edsjo A., Ehrnstrom R., Lindgren A., Ulmert D., Andersson T. and Bjartell A. 2011. Elevated level of Wnt5a protein in localized prostate cancer tissue is associated with better outcome. *PLoS One*. Vol. 6. Issue 10.
3. Banday A., Azim S. and Tabish M. 2011. Alternative promoter usage and differential expression of multiple transcripts of mouse Prkar1a gene. *Molecular and Cellular Biochemistry*. Vol. 357. Page 263 – 274
4. Bee T., Swiers G., Muroi S., Pozner A., Nottingham W., Santos A., Li PS., Taniuchi I. and Bruijin M. 2010. Nonredundant roles for *Runx1* alternative promoters reflect their activity at discrete stages of developmental hemotopoieses. *Blood*. Vol. 115.
5. Bilkovaski R., Schulte D., Oberhauser F., Gomolka M., Udelhove M., Hettich M., Roth B., Heidenreich A., Gutschow C., Krone W. and Laudes M. 2010. Role of Wnt-5a in the Determination of Human Mesenchymal Stem cells into Preadipocytes. *Journal of Biological Chemistry*. Vol. 285. No. 9
6. Binder C. and Pukrop T. 2008. The complex pathways of Wnt 5a in cancer progression. *Journal of Molecular Medicine*. Vol. 86. Page 259 – 266
7. Cheong J., Yamada Y., Yamashita R., Irie T. and Kanai A. 2006. Diverse DNA methylation statuses at alternative promoters of human genes in various tissues. *DNA Research*. Vol. 13. Page 155 – 167
8. Christodoulides C., Lagathu C., Sethi J. and Vidal-Puig A. 2008. Adipogenesis and WNT signaling. *Trends in Endocrinology and Metabolism*. Vol. 20. No. 1

9. Enomoto M., Hayakawa S., Itsukushima S., Ren D., Matsuo M., Tamada K., Oneyama C., Okada M., Takumi T., Nishita M. and Minami Y. 2009. Autonomous regulation of osteosarcoma cell invasiveness by Wnt 5a/Ror2 signaling. *Oncogene*. Vol. 28. Page 3197 – 3208
10. Roman-Gomez J., Jimenez-Velasco A., Agirre X., Castillejo J., Navarro G., Barrios M., Andreu E., Prosper F., Heiniger A. and Torres A. 2004. Transcriptional silencing of the Dickkopf-3 (Dkk-3) gene by CpG hypermethylation in acute lymphoblastic leukaemia. *British Journal of Cancer*. Vol. 91. Page 707–713
11. Katoh M and Katoh M. 2009. Transcriptional mechanisms of Wnt5a based on NF- κ B, hedgehog, TGF- α , and Notch signaling cascades. *International Journal of Molecular Medicine*. Vol. 23. Page 763 – 769
12. Nakano T., Tani M., Ishibashi Y., Kimura K., Park Y.B., Imaizumi N., Tsuda H., Aoyagi K., Sasaki H., Ohwad S. and Yokota J. 2003. Biological properties and gene expression associated with metastatic potential of human osteosarcoma. *Clinical & experimental Metastasis*. Vol. 20. Page 665 – 674
13. Nishita M., Enomoto M., Yamagata K. and Minami Y. 2010. Cell/tissue-tropic functions of Wnt5a signaling in normal and cancer cells. *Trends in Cell Biology*. Vol. 20. No. 6.
14. Nishizuka M., Koyanagi A., Shigehiro O. and Imagawa M. 2008. Wnt4 and Wnt5a promote adipocyte differentiation. *Rederation of European Biochemical Societies*. Vol. 582. Page 3201 – 3205
15. Jonsson M., Dejmek J., Bendahl P.O. and Andersson T. 2002. Loss of Wnt-5a protein is associated with early relapse in invasive ductal breast carcinomas. *Cancer Research*. Vol. 62. Page 409 – 416
16. McDonald S. and Silver A. 2009. The opposing roles of Wnt-5a in cancer. *British Journal of Cancer*. Vol. 101. Page 209 – 214
17. Michl P, Ramjaun AR, Pardo OE, Warne PH, Wagner M, Poulsom R., D'Arrigo C., Ryder K., Menke A., Gress T. and Downward J. 2005. CUTL1 is a target of TGF- β signaling that enhances cancer cell motility and invasiveness. *Cancer Cell*. Vol. 7. Page 521–532

18. Paina S., Garzotto D., DeMarchis S., Marino M., Moiana A., Conti L., Cattaneo E., Perera M., Corte G., Calautti E. and Merlo G. 2011. Wnt5a is a transcriptional target of Dlx homeogenes and promoter differentiation of interneuron progenitors in vitro and in vivo. *Journal of Neuroscience*. Vol. 7. Page 2675 – 2687
19. Roumiantsev S., Krause D., Neumann C., Dimitri C., Asiedu F., Corss N. and Van Etten R. 2004. Distinct stem cell myeloproliferative/T lymphoma syndromes induced by ZNF198-FGFR1 and BCR-FGFR1 fusion genes from 8p11 translocations. *Cancer Cell*. Vol.5. Page 287 – 298
20. Ripka S., Konig A., Buchholz M., Wagner M., Sipos B., Kloppel G., Downward J., Gress T.M. and Michl P. 2007. Wnt5a-target of Cutl1 and potent modulator of tumor cell migration and invasion in pancreatic cancer. *Carcinogenesis*. Vol. 28. No. 6. Page 1178 – 1187
21. Turner J., Pelascini L., Macedo J. and Muller C. 2008. Highly individual methylation patterns of alternative glucocorticoid receptor promoters suggest individualized epigenetic regulatory mechanisms. *Nucleic Acids Research*. Vol. 36. No. 22. Page 7202 – 7218
22. Wang Q., Williamson M., Bott S., Brookman-Amisshah N., Freeman A., Nariculam J., Hubank M., Ahmed A. and Masters J. 2007. Hypomethylation of Wnt5a, CRIP1 and S100P in prostate cancer. *Oncogene*. Vol. 26. Page 6560 – 6565
23. Wang Y. 2009. Wnt/Planar cell polarity signaling: A new paradigm for cancer therapy. *Molecular Cancer Therapeutics*. Vol. 8. Page 2103 – 2109
24. Weeraratna A., Jiang Y., Hostetter G., Rosenblatt K., Duray P., Bittner M. and Trent J. 2002. Wnt5a signaling directly affects cell motility and invasion of metastatic melanoma. *Cancer Cell*. Vol. 1. Page 279 – 288
25. Weinstein L., Xie T., Zhang Q.H. and Chen M. 2007. Studies of the regulation and function of the Gs alpha gene Gnas using gene targeting technology. *Pharmacol Ther*. Vol. 115. Page 271 – 291
26. Yamaguchi T.P., Bradley A., McMahon A.P. and Jones S. 1999. A Wnt5a pathway underlies outgrowth of multiple structures in the vertebrate embryo. *Development*. Vol. 126. Page 1211 – 1223